

# HucMSC-Exo Promote Mucosal Healing in Experimental Colitis by Accelerating Intestinal Stem Cells and Epithelium Regeneration via Wnt Signaling Pathway

Xiaonan Liang<sup>1,\*</sup>, Chenyang Li<sup>1,\*</sup>, Jia Song<sup>1</sup>, Airu Liu<sup>1</sup>, Chen Wang<sup>1</sup>, Wenxin Wang<sup>1</sup>, Yaxing Kang<sup>1,2</sup>, Donglei Sun<sup>1</sup>, Jiaming Qian<sup>1,3</sup>, Xiaolan Zhang<sup>1</sup>

<sup>1</sup>Department of Gastroenterology, The Second Hospital of Hebei Medical University, Hebei Key Laboratory of Gastroenterology, Hebei Institute of Gastroenterology, Hebei Clinical Research Center for Digestive Diseases, Shijiazhuang, Hebei, People's Republic of China;

<sup>2</sup>Department of Endocrinology, The Second Hospital of Hebei Medical University, Shijiazhuang, Hebei, People's Republic of China;

<sup>3</sup>Department of Gastroenterology, Peking Union Medical College Hospital, Chinese Academy of Medical Sciences and Peking Union Medical College, Beijing, People's Republic of China

\*These authors contributed equally to this work

Correspondence: Xiaolan Zhang, Department of Gastroenterology, The Second Hospital of Hebei Medical University, No. 215 Heping West Road, Shijiazhuang, Hebei, 050000, People's Republic of China, Tel +86 0311-66007370, Email xiaolanzh@hebmu.edu.cn; Jiaming Qian, Department of Gastroenterology, Peking Union Medical College Hospital, Chinese Academy of Medical Sciences and Peking Union Medical College, Beijing, 100730, People's Republic of China, Tel +86 010-69158100, Email qianjiaming1957@126.com

**Background:** Mucosal healing has emerged as a crucial therapeutic goal for inflammatory bowel diseases (IBD). Exosomes (Exo) as a potential acellular candidate for stem cell therapy might be competent to promote mucosal healing, while its mechanism remains unexplored.

**Methods:** Exosomes derived from human umbilical cord mesenchymal stem cells (hucMSCs) were subjected to experimental colitis mice intraperitoneally to estimate the role in mucosal healing and the regeneration of intestinal stem cells (ISCs) and epithelium. The intestinal organoid model of IBD was constructed utilizing tumor necrosis factor (TNF)- $\alpha$  for subsequent function analysis in vitro. Transcriptome sequencing was performed to decipher the underlying mechanism and Wnt-C59, an oral Wnt inhibitor, was used to confirm that further. Finally, the potential specific components of hucMSC-exo were investigated based on several existing miRNA expression datasets.

**Results:** HucMSC-exo showed striking potential for mucosal healing in colitis mice, characterized by decreased histopathological injuries and neutrophil infiltration as well as improved epithelial integrity. HucMSC-exo up-regulated the expression of leucine-rich repeat-containing G-protein coupled receptor 5 (Lgr5), a specific marker for ISCs and accelerated the proliferation of intestinal epithelium. HucMSC-exo endowed intestinal organoids with more excellent capacity to grow and bud under TNF- $\alpha$  stimulation. More than that, the fact that hucMSC-exo activated the canonical Wnt signaling pathway to promote mucosal healing was uncovered by not only RNA-sequencing but also relevant experimental data. Finally, bioinformatics analysis of the existing miRNA expression datasets indicated that several miRNAs abundant in hucMSC-exo involved widely in regeneration or repair related biological processes and Wnt signaling pathway might be one of the most important signal transduction pathways.

**Conclusion:** Our results suggested that hucMSC-exo could facilitate mucosal healing in experimental colitis by accelerating ISCs and intestinal epithelium regeneration via transferring key miRNAs, which was dependent on the activation of Wnt/ $\beta$ -catenin signaling pathway.

**Keywords:** inflammatory bowel disease, mesenchymal stem cells, exosome, mucosal healing, Wnt/ $\beta$ -catenin signaling pathway

## Introduction

The inflammatory bowel diseases, typically categorized as ulcerative colitis and Crohn's disease, are chronic non-specific intestinal disorders.<sup>1</sup> Although the lack of a comprehensive understanding of its underlying pathophysiological mechanisms, it is widely accepted that the interplay between genetic susceptibility, environmental factors and microbial dysbiosis, which mediates dysregulated immune responses, results in the relapsing intestinal inflammation and prolonged mucosal damage.<sup>2</sup>

Mucosal healing associated with the improved long-term outcomes in IBD has emerged as a crucial therapeutic goal.<sup>3</sup> Given the prominent role of immune anomalism in IBD, the current armamentarium including untargeted therapies, such as 5-aminosalicylate, glucocorticoids and immunomodulators, as well as targeted biologic therapies, such as anti-TNF agents, anti-integrin  $\alpha 4\beta 7$  antibody and anti-IL12/23 p40 antibody, even the novel small-molecule Janus kinase inhibitor all aims to regain the immunological homeostasis, but fails to promote mucosal healing satisfactorily with only 30–50% mucosal improvements.<sup>4–7</sup> Hence, there has been a growing recognition that mucosal healing based on the intact barrier function of the gut epithelium, which can prevent the translocation of commensal bacteria or hazardous substances into the mucosa or deeper with subsequent immune cell activation, should be considered as an initial event in the suppression of gut inflammation, rather than a sign of complete inflammation resolution.<sup>8</sup> So, further exploration of new therapeutic strategies is imminent and imperative to break through the “mucosal healing ceiling”.

Mesenchymal stem cells with both robust immunomodulatory capacity and enormous regenerative potential have gradually become a promising candidate in the field of regenerative medicine,<sup>9,10</sup> which demonstrated striking therapeutic effects in autoimmune diseases<sup>11</sup> and has been a novel paradigm for the treatment of IBD.<sup>12</sup> Exosomes are secreted membrane-enclosed vesicles with a size range of 40–160 nm in diameter.<sup>13,14</sup> Exosomes serving as important mediators of intercellular communication, which can be released by all cell types, contain diverse constituents of their cell of origin and exhibit similar biological activity to the parent cell.<sup>14</sup> Exosomes derived from MSCs have been demonstrated as a stepping-stone for their therapeutic effects<sup>15,16</sup> and could be a potential acellular alternative for stem cell therapy. Accumulating evidences have demonstrated that exosomes derived from MSCs could ameliorate experimental colitis significantly, while the vast majority of them dedicated to explore the immunomodulatory function rather than regenerative capacity.<sup>17,18</sup> We previously reported that hucMSC-exo could not only regulate the immune homeostasis but also enhance intestinal barrier function.<sup>19</sup> Nevertheless, the mechanism by which hucMSC-exo mediates mucosal healing remains unclear, such as the underlying signal transduction pathway and the potential functional components.

In the present study, we confirmed the therapeutic effect of hucMSC-exo in both dextran sulfate sodium (DSS)- and 2,4,6-trinitrobenzenesulfonic acid (TNBS)-induced colitis model as well as intestinal organoids stimulated by TNF- $\alpha$ . Furthermore, we shed light on the molecular mechanism underlying the facilitation on mucosal healing by promoting the regeneration of Lgr5<sup>+</sup> ISC and intestinal epithelium with the aid of transcriptome sequencing technologies, and identified its potential specific components by public data acquisition and analysis. These findings might provide a new therapeutic strategy targeting mucosal healing directly and open new avenues for acellular regenerative medicine in IBD.

## Materials and Methods

### Isolation and Characterization of hucMSC-Exosomes

HucMSCs were provided by Shandong Qilu cell therapy Engineering Technology Co., Ltd. For hucMSC-exo extraction, hucMSCs at 3–5 passages were used according to our previously described methods.<sup>19</sup> Briefly, hucMSCs culture supernatant was collected and centrifuged at 3000 g for 15 min to remove dead cells and cell debris. The resultant supernatant was filtered once through 0.22  $\mu$ m pore filter (Merck KGaA, Darmstadt, Germany) to eliminate cell debris and bacteria. The filtered supernatant was concentrated with a 150-kD Protein Concentrator (Millipore, Massachusetts, USA) and filtered once again using 0.22- $\mu$ m pore filter to eliminate bacteria further. The final supernatant was subject to ExoQuick-TC exosome isolation reagent (5: 1, v/v; System Biosciences, California, USA) and incubated at 4°C for 12

h. Then, the exosomes pellet was collected after centrifuging at 15,000 g for 30 min and resuspended in PBS. Finally, it was stored at  $-80^{\circ}\text{C}$  after quantified the protein concentration by the BCA method.

For characterization, hucMSC-exo were detected using transmission electron microscopy (TEM) to observe the morphology and size. Particle size distribution was assessed by flow nano-Analyser (NanoFCM, Xiamen, China). Finally, the typical exosomal markers were validated by Western blot. Detailed procedures are provided in [Supplementary Materials](#).

## Animal Model Establishment and hucMSC-Exosomes Treatment

All animal experiments were approved by the Research Ethics Committee of the Second hospital of Hebei Medical University and conducted in strict conformity with China's Guidelines for the Ethical Review of Laboratory Animal Welfare. Male C57BL/6 and BABL/c mice (6–8 weeks, 18–22 g) of specific-pathogen-free (SPF) grade were purchased from Beijing Vital River Laboratory Animal Technology Co. Ltd. and housed in an SPF environment.

The mice were divided into control, model and treatment group in accordance with the random number table. In DSS-induced colitis model, mice were provided with 2% (m/v) DSS (MP Biomedicals, California, USA) for 7 consecutive days ad libitum and autoclaved drinking water for the following 3 days. Starting from the 4th day, the DSS-EXO group received injections of 300  $\mu\text{g}$  hucMSC-exo in 200  $\mu\text{L}$  PBS every other day intraperitoneally, and the DSS+PBS group received PBS for vehicle control. In TNBS-induced colitis model, mice were pre-sensitized with 1% TNBS (Sigma-Aldrich, USA) for 7 days prior to enema, then subjected to 100  $\mu\text{L}$  3% TNBS transrectally, and 40% ethanol solution was used as vehicle control. For treatment, 300  $\mu\text{g}$  hucMSC-exo was administrated via intraperitoneal injection on the 1st and 3rd day. The Wnt signaling pathway inhibition experiment was conducted based on the DSS-induced colitis model utilizing a highly potent and oral Wnt inhibitor, Wnt-C59. Briefly, Wnt-C59 (10 mg/kg) was orally administered beginning on the 4th day and continued for the remaining 5 days daily, equal volume of DMSO was used as vehicle control.<sup>20</sup>

Mice survival, general condition, body weight, diarrhea and hematochezia were monitored daily throughout the duration of the experiment. The disease activity index (DAI) scores of each mouse were recorded everyday according to the standard protocol with slight modifications ([Supplementary Table 1](#)).<sup>21</sup> Mice were anesthetized and sacrificed at the time points of choice, then the colon tissues were harvested for subsequent experiments. The animals were excluded if they died prematurely, affecting the collection of histological data.

## The Construction of Experimental Colitis Model Utilizing Intestinal Organoids

The intestinal crypt isolation and organoid culture were performed according to the manufacturer's instructions based on Hans Clevers protocol.<sup>22</sup> In brief, small intestinal tissue was harvested and washed in cold Dulbecco's phosphate-buffered saline (DPBS) thoroughly, then cut into 2-mm fragments. Crypt suspension was collected after incubation of intestinal fragments in Gentle Cell Dissociation Reagent (GCDR) (Stemcell Technologies, Canada) for 15 min at room temperature. After filtering through 70 $\mu\text{m}$  cell strainer and centrifuging sequentially (290 g  $\times$  5 min, 200 g  $\times$  3 min), the purified crypts were obtained. Next, crypts resuspended in the mixture of appropriate IntestiCult™ Organoid Growth Medium (STEMCELL Technologies, Canada) and equal volume of Phenol-red free, reduced growth factor Matrigel (Corning, USA) were seeded in a preheated 24-well plate with 50  $\mu\text{L}$  per well. Finally, 600  $\mu\text{L}$  culture medium was added into each well after Matrigel polymerized utterly and the intestinal organoids were cultured at  $37^{\circ}\text{C}$ , 5%  $\text{CO}_2$  with the medium refreshed every other day.

To mimic the inflammatory environment in vitro, TNF- $\alpha$  was added into the complete medium to a final concentration of 50 ng/mL as previously described with slight modifications,<sup>23–25</sup> DMSO was used as vehicle control. Meanwhile, 100  $\mu\text{g}/\text{mL}$  hucMSC-exo were administrated continuously for 48 h to evaluate the efficacy ex vivo.

## Hematoxylin and Eosin Staining (H&E)

The distal colon tissues were submitted for histopathological processing, which were fixed adequately in formaldehyde, then manufactured for paraffin sections, stained with hematoxylin and eosin (H&E) ultimately. Inflammation, extent,

regeneration, crypt damage and percent involvement were assessed at the light microscopic level, and quantitated using Dieleman score system with slight modifications ([Supplementary Table 2](#)).<sup>26</sup>

## Myeloperoxidase (MPO) Activity Assay

MPO activity can be measured spectrophotometrically with the MPO assay kit (Nanjing Jiancheng Bioengineering Institute, Nanjing, China), to evaluate neutrophil infiltration quantitatively. MPO activity was expressed as units per gram of total protein (U/g).<sup>19</sup>

## Intestinal Permeability Assay

Intestinal mucosal permeability was evaluated as we previously reported using fluorescein isothiocyanate-dextran (FITC-D, 4 kDa; Sigma-Aldrich, St. Louis, USA).<sup>19</sup> In brief, mice were fed with FITC-D (60 mg/100 g) 4 h before sacrifice. The serum samples were collected, then serum FITC-D fluorescence was detected by fluorescence spectrophotometer at an excitation wavelength of 490 nm and an emission wavelength of 520 nm. At length serum FITC-D concentrations were calculated according to the standard curve.

## RNA Isolation and Real-Time PCR

The mRNA expressions of inflammatory cytokines and *Lgr5* were detected by real-time PCR as described previously.<sup>19</sup> All primer sequences are listed in [Supplementary Table 3](#). GAPDH was used as an internal standard. The  $2^{-\Delta\Delta C_t}$  method was employed to quantify the relative gene expression levels.

## Protein Extraction and Western Blot

Western blot was conducted to detect the protein expressions of the exosome surface markers, the ISCs marker *Lgr5* and the key proteins of Wnt signaling pathway. The detailed protocol was described previously.<sup>19</sup> Equal amounts of proteins (20 µg/lane for exosomes protein; 75 µg/lane for colon tissue protein) were separated by SDS-PAGE gel and then transferred to 0.22 µm PVDF membranes. After being blocking by 5% fat-free milk, the membranes with separated proteins were incubated with primary antibodies overnight at 4°C, rinsed by Tris buffered saline with Tween-20 (TBST) and then incubated with secondary antibodies (1: 10,000, Cat#C50331-05, LI-COR, Lincoln, NE, USA) for 1h at room temperature sequentially. The protein bands were visualized and analyzed using the Odyssey CLx imaging systems (LI-COR, Lincoln, NE, USA). Anti-CD9 (1: 1000, Cat#ab92726, Abcam, Cambridge, UK), anti-CD63 (1: 1000, Cat#ab134045, Abcam, Cambridge, UK), anti-TSG101 (1: 1000, Cat#ab125011, Abcam, Cambridge, UK), anti-Calnexin (1: 1000, Cat#ab133615, Abcam, Cambridge, UK), anti-LGR5 (1: 1000, Cat#ab75850, Abcam, Cambridge, UK), anti-WNT2 (1: 500, Cat#CY5299, Abways, Shanghai, China), anti-non-phospho (Active) β-Catenin (Ser33/37/Thr41) (1: 1000, Cat#8814, CST, MA, USA), anti-β-Catenin (1: 1000, Cat#CY3523, Abways, Shanghai, China) antibodies were used as primary antibodies, respectively. The protein expression was normalized to β-actin (1: 2000, Cat#AB0035, Abways, Shanghai, China) or GAPDH (1: 2000, Cat#AB0037, Abways, Shanghai, China).

## Immunohistochemical Staining

The neutrophil infiltration and epithelium proliferation potential in the remaining crypts were severally visualized by the MPO and Ki-67 immunohistochemical staining as described in previous study.<sup>27,28</sup> Briefly, the colon tissue sections were incubated with primary anti-MPO (1: 1000, Cat#ab208670, Abcam, Cambridge, UK) or anti-Ki-67 (1: 200, Cat#ab16667, Abcam, Cambridge, UK) antibodies at 4°C overnight, and detected given antibodies by corresponding biotin–streptavidin–peroxidase procedure with diaminobenzidine as the chromogen. Then, sections were scanned using CX40 optical microscope (Olympus, Tokyo, Japan) and the positive staining cells were analyzed.

## Immunofluorescence (IF) Staining

The distribution of Ki-67 positive cells in intestinal organoids and active β-catenin in colon tissues were visualized and semi-quantitated by Immunofluorescence staining as previously reported with minor modifications.<sup>29,30</sup> Intestinal organoids were incubated with anti-Ki-67 (1: 50, Cat#ab16667, Abcam, Cambridge, UK) antibodies and corresponding



fluorescence secondary antibody (1: 50, Cat#AB0151, Abways, Shanghai, China). Colonic tissue sections were subjected to a similar protocol with anti-active  $\beta$ -Catenin (1: 400, Cat#8814, CST, MA, USA) as primary antibody. DAPI (Beyotime, Shanghai, China) was used for nucleus counterstaining. At last, sections were scanned with the laser scanning confocal microscope FV12-IXCOV (Olympus, Tokyo, Japan) and analyzed by Image J software.

## EdU Incorporation Assay

EdU incorporation assay was performed to assess epithelium regeneration using EdU-488 Proliferation Detection Kit (Beyotime, Shanghai, China). For the in vivo assay, mice were labeled with 100 mg/kg EdU via intraperitoneal injection, then sacrificed 4 h after the injection. For the ex-vivo assay, intestinal organoids were incubated in the complete medium supplemented with 20  $\mu$ M EdU at 37°C for 120 min, then harvested for subsequent experiments. Finally, the relative fluorescent intensity of EdU versus DAPI and EdU<sup>+</sup> cells per crypt was analyzed.

## RNA Sequencing

This section was accomplished by Shanghai Biotechnology Corporation. Total RNA was extracted using the TransZol Up Plus RNA Kit (TransGen Biotech, Beijing, China), checked for RNA integrity by an Agilent 2100 Bioanalyzer (Agilent Technologies, Santa Clara, CA, US), then purified using RNAClean XP Kit (Cat A63987, Beckman Coulter, Brea, CA, USA) and RNase-Free DNase Set (QIAGEN, GmbH, Germany). Next, cDNA libraries were generated using the VAHTS Universal V6 RNA-seq Library Prep Kit for Illumina (Vazyme, Nanjing, China) and sequenced using the Illumina NovaSeq6000 (Illumina, San Diego, CA, USA) as per the manufacturer's recommendations. The raw reads were filtered by Seqtk before mapping to genome using Hisat2 (version: 2.0.4). The fragments of genes were counted using stringtie (v1.3.3b) followed by TMM (trimmed mean of M values) normalization. Significant differential expressed genes (DEGs) were identified as those with a False Discovery Rate (FDR) value above the threshold ( $Q \leq 0.05$ ) and fold-change  $\geq 2$  using edgeR software. Finally, gene ontology (GO) and Kyoto Encyclopedia of Genes and Genomes (KEGG) enrichment analysis were performed and further characteristic gene signatures were applied for Gene set enrichment analysis (GSEA) using the clusterProfiler package of R.

## Public Data Acquisition and Bioinformatic Analysis

The existing hucMSC-exo miRNA expression profile datasets were downloaded from Gene Expression Omnibus (GEO, GSE69909 and GSE159814, all from <https://www.ncbi.nlm.nih.gov/geo/>) and additional file from Yi Zhang's article (<https://stemcellres.biomedcentral.com/articles/10.1186/s13287-021-02159-2>).<sup>31</sup> GSE46989 was also downloaded to explore the miRNA expression patterns in hucMSCs. The top 20 miRNAs expressed in hucMSCs or hucMSC-exo were selected. TargetScan,<sup>32</sup> miRDB<sup>33</sup> and TarBase<sup>34</sup> were used to predict the target genes of miRNAs enriched in hucMSCs. All predicted targets were subjected to GO and KEGG analysis by DAVID<sup>35,36</sup> online with default setting to decipher the potential mechanism of candidate hucMSC-exo miRNAs during mucosal healing in IBD.

## Statistical Analysis

Data were presented as the mean  $\pm$  SD. Mouse survival curves were plotted by the Kaplan–Meier method and analyzed by Log rank test. The Mann–Whitney *U*-test (non-normal distribution) or Unpaired Student's *t*-test (normal distribution) was used to compare the variables between two groups.  $P < 0.05$  was considered as statistically significant. Statistical analysis was performed using SPSS 22.0.

## Results

### Characterization of hucMSC-Exosomes

The isolated hucMSC-exo were characterized by different methods including TEM, NanoFCM, and Western blot. HucMSC-exo showed a typically cup-shaped morphology with diameter of about 90 nm ([Supplementary Figure 1A and B](#)). Western blot showed that hucMSC-exo expressed exosome-specific markers such as CD9, CD63, TSG101, but not calnexin ([Supplementary Figure 1C](#)).

## HucMSC-Exosomes Promote Mucosal Healing in Experimental Colitis Mice

DSS-induced colitis model was constructed to investigate the therapeutic effects of hucMSC-exo on inflammatory bowel disease (Figure 1A). The survival status, body weight and feces of mice were observed daily. There was only 50% survival in experimental colitis mice, while administration of hucMSC-exo improved survival to 86% (Figure 1B). Moreover, hucMSC-exo prevented serious weight loss (Figure 1C) and hematochezia, thus decreased the DAI scores (Figure 1D). On the 10th day after modeling, mice in DSS+Exo group exhibited longer colon length (Figure 1E and F) along with lower histopathological score which represented a degree of mucosal healing, reduced crypt loss, improved epithelial integrity and subdued inflammatory cell infiltration (Figure 1G and [Supplementary Figure 2](#)). Meanwhile, both the IHC staining of MPO and colorimetric assay for MPO activity indicated that neutrophil infiltration was reduced in hucMSC-exo treated mice (Figure 1H and I). The determination of serum FITC-D concentration demonstrated that hucMSC-exo maintained the integrity of intestinal mucosa by reducing intestinal permeability (Figure 1J). And, cytokine analysis (Figure 1K) in mouse colon tissues presented that hucMSC-exo significantly promoted the production of anti-inflammatory mediator *Interleukin (Il)10*, while reduced the pro-inflammatory factors *Il17*, *Interferon gamma (Ifng)* and *Tnfa*. Not only that, the similar therapeutic effects were observed in TNBS-induced colitis mice although no mortality differences were noted in mice between TNBS+PBS group and TNBS+EXO group (Figure 2A–K and [Supplementary Figure 3](#)).

## HucMSC-Exosomes Contribute to Intestinal Stem Cells and Epithelium Regeneration in Colitis Mice

Mucosal healing is a complex process involving epithelium regeneration and migration, while the ISCs residing at the crypt base appear to be the “workhorse” of daily intestinal self-renewal and pathological regeneration.<sup>37</sup> To further explore the role of ISCs and epithelium in mucosal healing accelerated by hucMSC-exo, several ISCs and proliferation-related markers were detected in both DSS- and TNBS-induced colitis model. PCR and Western blot analysis revealed that hucMSC-exo significantly increased the expression of *Lgr5* at both mRNA and protein level (Figure 3A and B, [Supplementary Figure 4](#)). Simultaneously, hucMSC-exo improved the proliferative ability of intestinal epithelium which was determined by Ki-67 staining and EdU incorporation assay (Figure 3C and D, [Supplementary Figure 5A](#) and B). Collectively, hucMSC-exo could facilitate the regeneration of ISCs and intestinal epithelium to attenuate experimental colitis.

## HucMSC-Exosomes Facilitate Intestinal Stem Cells and Epithelium Regeneration in Organoid Model of Experimental Colitis

The development of 3D organoid technology opened a new era for the construction of disease models in vitro, which might be more representative of the in vivo situation. In order to reveal the effect of hucMSC-exo on ISCs and intestinal epithelium in vitro, we constructed intestinal organoid model for experimental colitis using TNF- $\alpha$ . Briefly, on the 3rd day after intestinal crypts seeding, TNF- $\alpha$  (50 ng/mL) was added into the complete medium accompanied by hucMSC-exo (100  $\mu$ g/mL). The results showed that TNF- $\alpha$  stimulation attenuated the growth rate, budding rate and average buddings number at 48 h, while hucMSC-exo reversed the suppression induced by TNF- $\alpha$  partially which implied hucMSC-exo contribute to ISCs regeneration in vitro (Figure 4A–D). In addition, the epithelium in the hucMSC-exo treatment organoids also showed greater regeneration potential, characterized by a prominent increase in the percentage of Ki-67 positive cells and EdU incorporation (Figure 4E and F).

## HucMSC-Exosomes Activate the Wnt/ $\beta$ -Catenin Signaling Pathway in Experimental Colitis

As stem cell fate is largely determined by the complex microenvironment, the intricate cell signaling network, including Wnt, Notch, Hippo, epidermal growth factor (EGF), bone morphogenetic protein (BMP) signaling and so on, plays a pivotal role in the regulation of plasticity and ISCs function during mucosal healing.<sup>38</sup> To elucidate the underlying molecular mechanisms by which hucMSC-exo promoted mucosal healing via the modulation of ISCs function, RNA

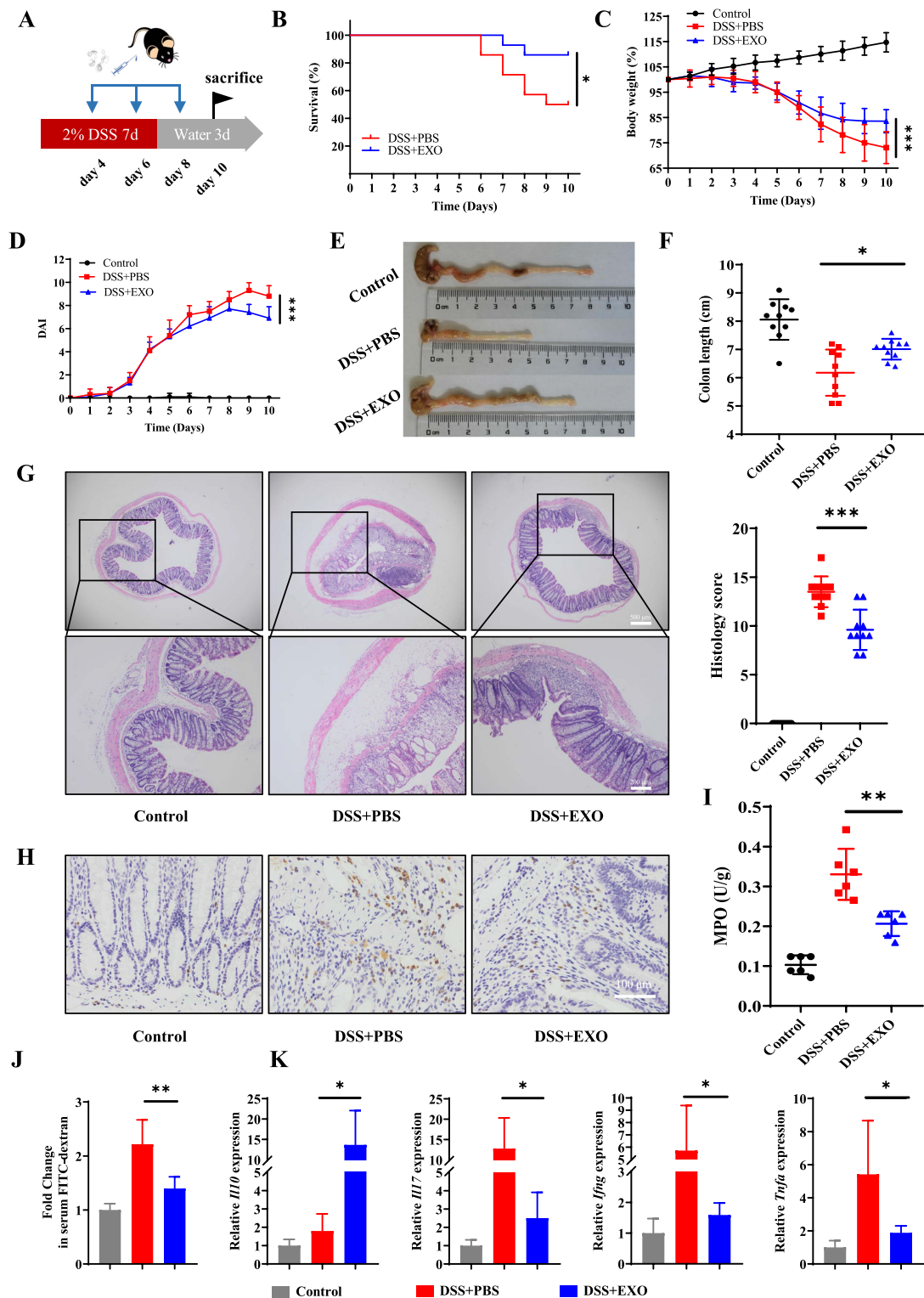


**Figure 1** HucMSC-exo accelerated mucosal healing in DSS-induced colitis mice. **(A)** Schematic diagram for the construction of DSS-induced colitis model and hucMSC-exo treatment. **(B)** The survival curves of mice in DSS-induced colitis model (n refers to the number of animals in each group, n=14). **(C)** Changes in mice weight (n=10). **(D)** DAI scores of mice (n=10). **(E)** Macroscopic images of colon tissues. **(F)** Colon length in different groups (n=10). **(G)** H&E staining and histological scores of mice colon sections in DSS-induced colitis model (n=10, scale bar=500  $\mu$ m, 40 $\times$ ; scale bar=200  $\mu$ m, 100 $\times$ ). **(H)** The neutrophil infiltration in colon tissues measured by IHC staining of MPO (n=5, scale bar=100  $\mu$ m, 400 $\times$ ). **(I)** MPO activity in colon tissues evaluated by colorimetry (n=6). **(J)** Fold change in serum FITC-dextran between each group showing the intestinal permeability (n=6). **(K)** mRNA levels of *Il10*, *Il17*, *Ifng* and *Tnfa* in colon tissues estimated by real-time PCR (n=5). Data are presented as mean  $\pm$  SD. Mouse survival curves were plotted by the Kaplan–Meier method and analyzed by Log rank test. The Mann–Whitney U-test (non-normal distribution) or Unpaired Student's t-test (normal distribution) was used to compare the variables between two groups. P<0.05 was considered as statistically significant. \*P<0.05, \*\*P<0.01 and \*\*\*P<0.001.

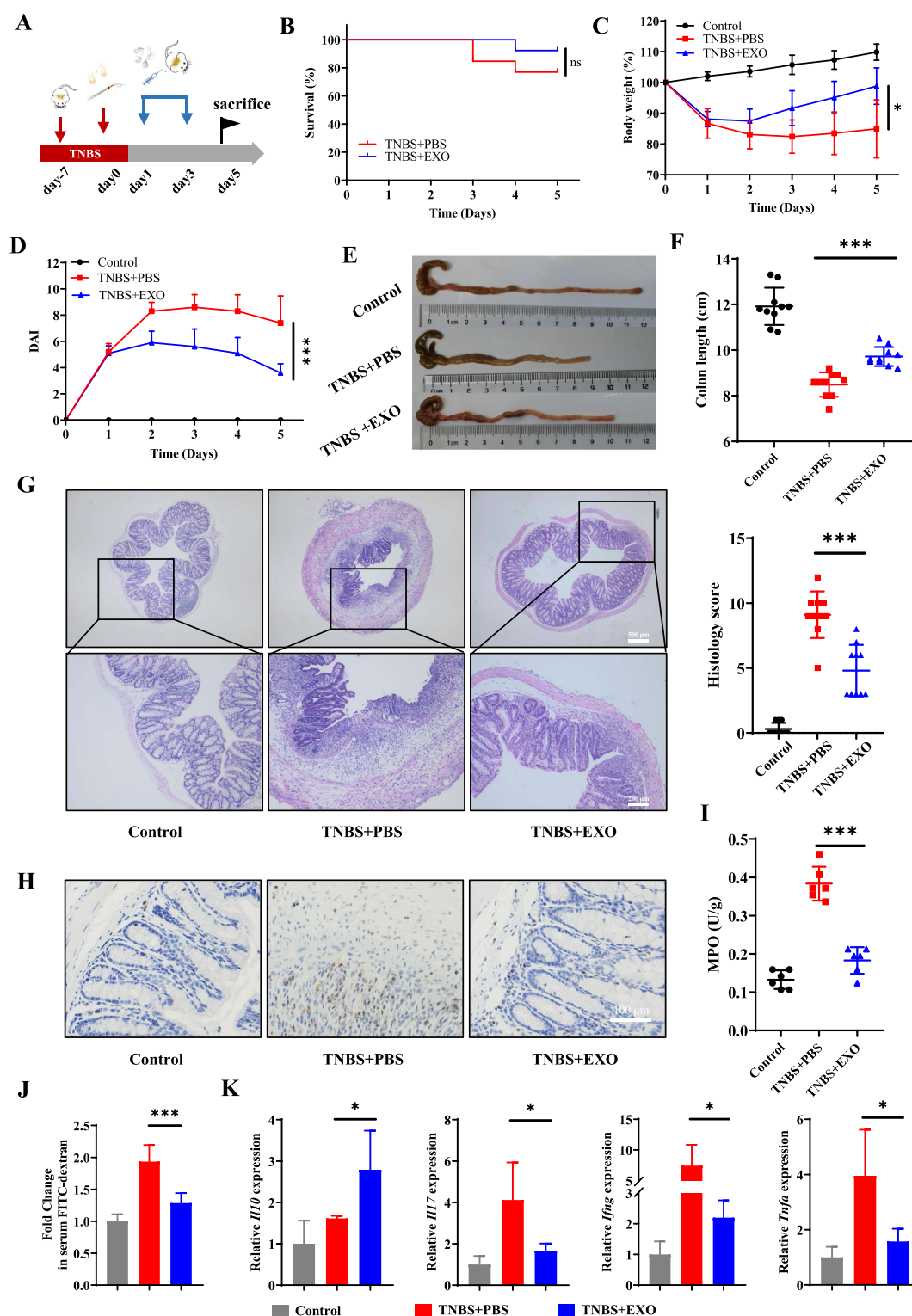


**Figure 2** HucMSC-exo accelerated mucosal healing in TNBS-induced colitis mice. **(A)** Schematic diagram for the construction of TNBS-induced colitis model and hucMSC-exo treatment. **(B)** The survival curves of mice in TNBS-induced colitis (n=13). **(C)** Changes in mice weight (n=10). **(D)** DAI scores of mice (n=10). **(E)** Macroscopic images of colon tissues. **(F)** Colon length in different groups (n=10). **(G)** H&E staining and histological scores of mice colon sections in TNBS-induced colitis model (n=10, scale bar=500  $\mu$ m, 40 $\times$ ; scale bar=200  $\mu$ m, 100 $\times$ ). **(H)** The neutrophil infiltration in colon tissues measured by IHC staining of MPO (n=5, scale bar=100  $\mu$ m, 400 $\times$ ). **(I)** MPO activity in colon tissues evaluated by colorimetry (n=6). **(J)** Fold change in serum FITC-dextran between each group showing the intestinal permeability (n=6). **(K)** mRNA levels of *Il10*, *Il17*, *Ifng* and *Tnfa* in colon tissues estimated by real-time PCR (n=5). Data are presented as mean  $\pm$  SD. Mouse survival curves were plotted by the Kaplan-Meier method and analyzed by Log rank test. The Mann-Whitney U-test (non-normal distribution) or Unpaired Student's t-test (normal distribution) was used to compare the variables between two groups. P<0.05 was considered as statistically significant. \*P<0.05 \*\*\*P<0.001 and ns indicates P>0.05.



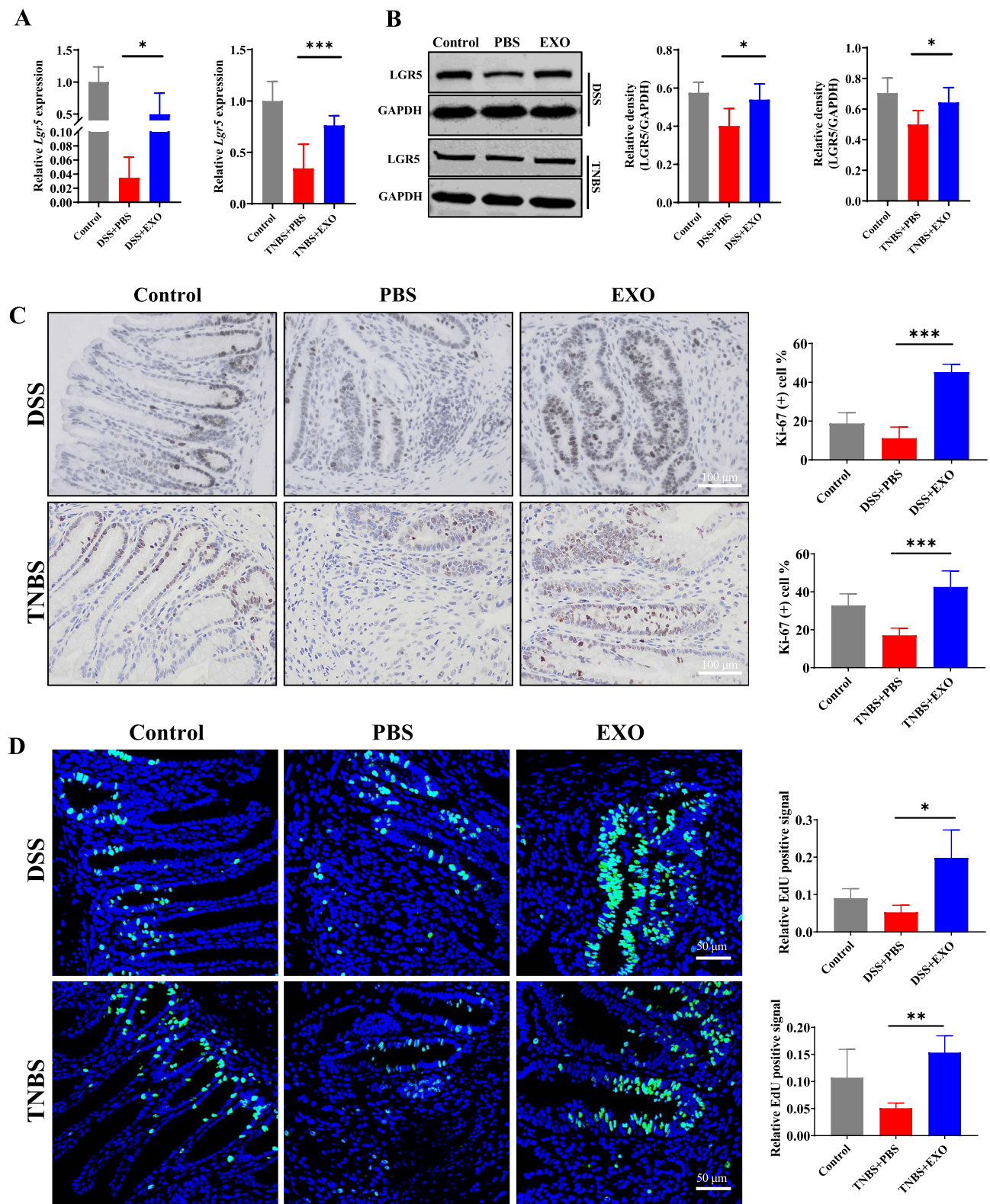


**Figure 3** HucMSC-exo promoted the regeneration of intestinal stem cells and epithelium in experimental colitis mice. **(A and B)** The mRNA and protein expression levels of ISCs marker *Lgr5* in colon tissues from indicated groups estimated by real-time PCR or Western blot respectively (n=5, corresponding full-length blots are presented in [Supplementary Figure 4](#)). **(C)** The proliferation potential of the remaining colon epithelium was measured by IHC staining of Ki-67 (n=5, scale bar=100  $\mu$ m, 400 $\times$ ). **(D)** Detected cell proliferation at the level of DNA synthesis by EdU incorporation assay (n=5, scale bar=50  $\mu$ m, 400 $\times$ ). Data were shown as mean  $\pm$  SD. The Mann–Whitney U-test (non-normal distribution) or Unpaired Student's *t*-test (normal distribution) was used to compare the variables between two groups.  $P < 0.05$  was considered as statistically significant. \* $P < 0.05$ , \*\* $P < 0.01$ , \*\*\* $P < 0.001$ .



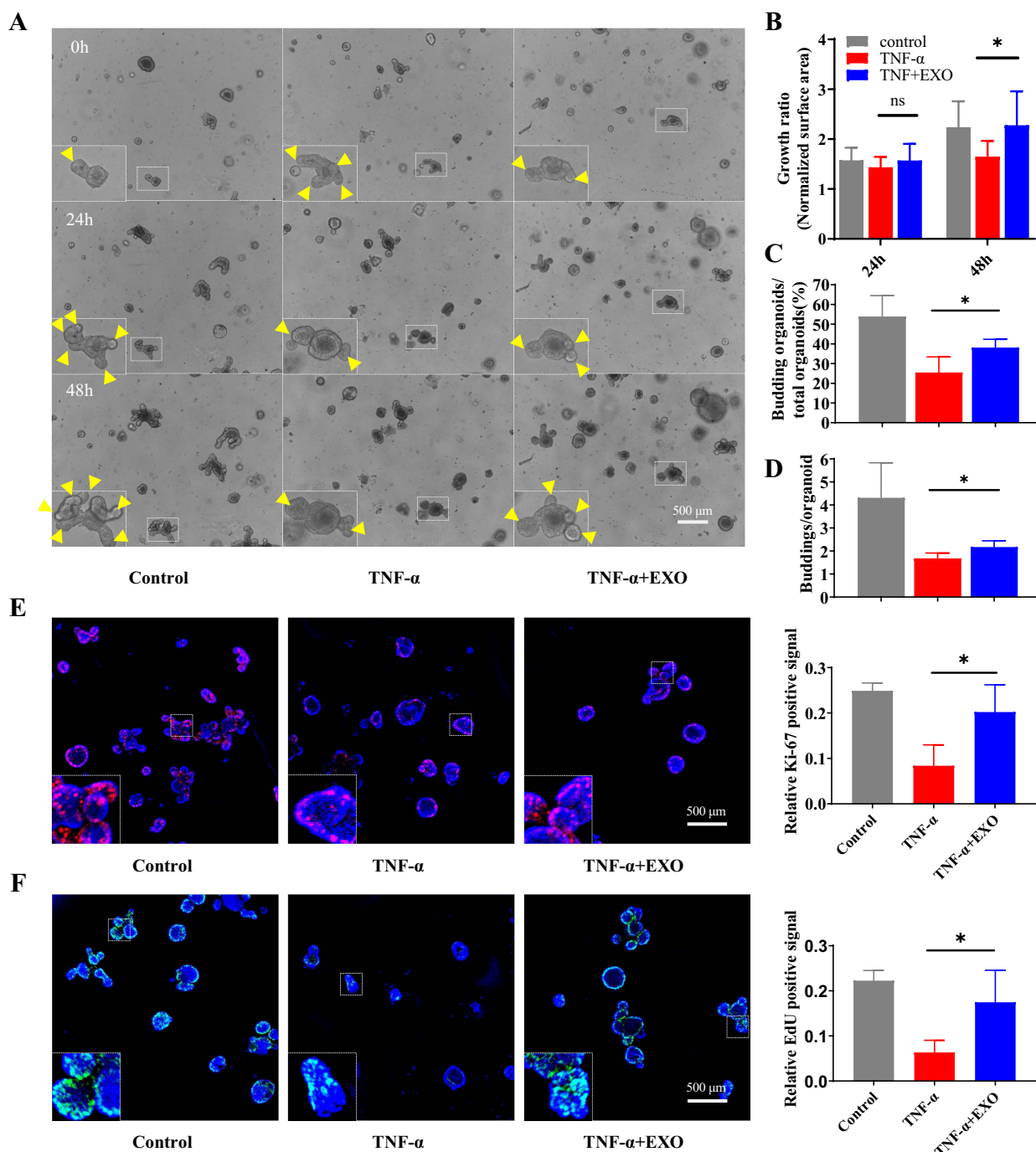


**Figure 4** HucMSC-exosomes promoted the regeneration of ISC and intestinal epithelium in organoids in ex-vivo colitis model. 100  $\mu$ g/mL hucMSC-exo were administrated continuously for 48 h to evaluate its effects on intestinal organoids. **(A–D)** The regeneration of ISCs was measured by organoid growth rate (24 h and 48 h, n refers to the number of organoids we consecutively observed in each group, n=8), budding rate (48 h) and average buddings number (48 h, n refers to the number of independent experiments, n=4). Yellow triangles marked buddings in organoid, scale Bar=500  $\mu$ m, 50 $\times$ . **(E and F)** The proliferation potential of epithelium in organoids was measured by IF staining of Ki-67 and EdU incorporation assay (48 h, n=4, scale Bar=500  $\mu$ m, 40 $\times$ ), results were expressed as the ratio of the integrated density of Ki-67 (red) or EdU (green) to DAPI (blue). Data were shown as mean  $\pm$  SD. The Mann–Whitney U-test (non-normal distribution) or Unpaired Student's t-test (normal distribution) was used to compare the variables between two groups.  $P < 0.05$  was considered as statistically significant. \* $P < 0.05$  and ns indicates  $P > 0.05$ .

sequencing of colon tissues in DSS-induced colitis model was performed. RNA-seq analysis revealed that 2035 up-regulated and 3203 down-regulated genes were identified (Figure 5A). The enrichment analysis revealed that the above DEGs were significantly enriched in GO terms related to mucosal healing, such as “wound healing”, “tissue remodeling”, “stem cell proliferation”, “stem cell differentiation”, “epithelial cell proliferation” and “epithelial cell migration”. And

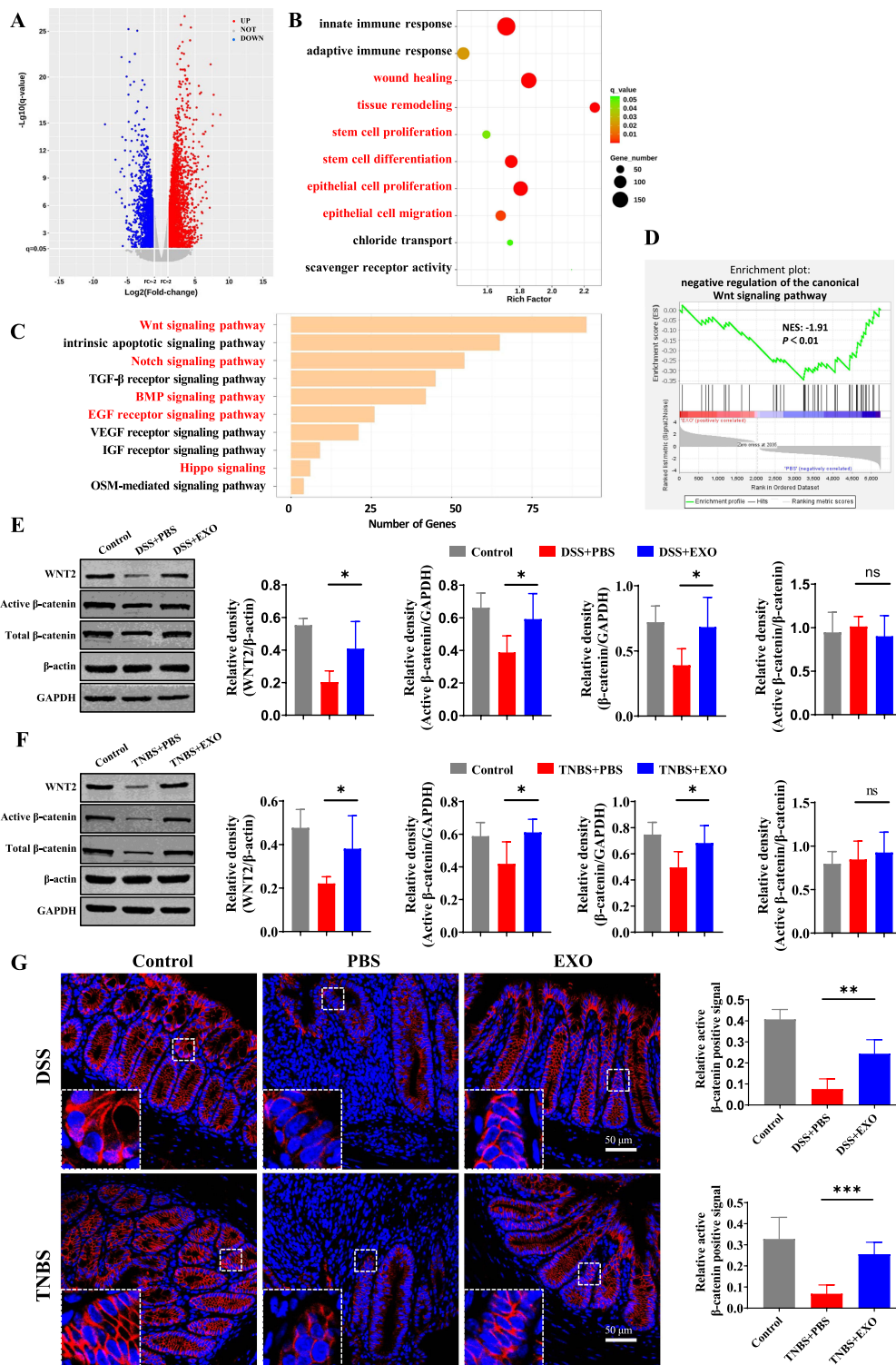


**Figure 5** HucMSC-exosomes activated the Wnt/ $\beta$ -catenin signaling pathway in experimental colitis mice. The mRNA of colon tissues from 5 mice in DSS+PBS group and 5 mice in DSS+EXO group were enrolled for RNA sequencing. **(A)** Volcano map of differentially expressed genes (DEGs) with  $p \leq 0.05$  and fold change  $\geq 2$ . **(B)** Enriched biological processes for genes in DSS+EXO group versus DSS+PBS group. **(C)** Enriched pathways associated with ISCs regeneration and mucosal healing. **(D)** Gene set enrichment analysis. NES, normalized enrichment score. It is generally considered that the gene set under the pathway of  $|NES| > 1$  is meaningful. **(E and F)** The protein expressions level of WNT2, active  $\beta$ -catenin and total  $\beta$ -catenin were analyzed by Western blot ( $n=5$ , corresponding full-length blots are presented in [Supplementary Figure 4](#)). **(G)** The localization and expression of active  $\beta$ -catenin (red) was analyzed by IF staining of active  $\beta$ -catenin ( $n=5$ , scale bar=50  $\mu\text{m}$ , 400 $\times$ ). The purple region produced by the mixture of red and blue (DAPI) was thought to be the place where  $\beta$ -catenin entered the nucleus. Data were shown as mean  $\pm$  SD. The Mann–Whitney U-test (non-normal distribution) or Unpaired Student's  $t$ -test (normal distribution) was used to compare the variables between two groups.  $P < 0.05$  was considered as statistically significant. \* $P < 0.05$ , \*\* $P < 0.01$ , \*\*\* $P < 0.001$ , ns indicates  $P > 0.05$ .

the most highly enriched pathway which could target the largest number of DEGs, “the canonical Wnt signaling pathway” was suppressed in DSS+PBS group (Figure 5B–D). That said hucMSC-exo activated Wnt/ $\beta$ -catenin signaling pathway according to RNA-seq and the DEGs enrichment analysis.

To verify the above results, WNT2, the significantly upregulated Wnt ligand according to RNA-seq analysis, and  $\beta$ -catenin were detected meticulously. As shown in Figure 5E and F, the protein expression levels of WNT2 in hucMSC-exo treatment group were significantly higher. As for  $\beta$ -catenin, although there was no difference in the ratio of active to total  $\beta$ -catenin, the hucMSC-exo dramatically increased the expression of total and active  $\beta$ -catenin and upregulated the nuclear  $\beta$ -catenin<sup>+</sup> cells notably (Figure 5E–G).

## The Effects of hucMSC-Exosomes on Alleviating Mucosal Healing Depend on the Activation of Wnt/ $\beta$ -Catenin Signaling Pathway

To further confirm the effects of hucMSC-exo via the activation of Wnt/ $\beta$ -catenin pathway, Wnt-C59, a highly potent and oral Wnt inhibitor, was administered to mice for 6 consecutive days (Figure 6A). There was no marked difference regarding survival rate between DSS+EXO group and DSS+EXO+Wnt-C59 group (Figure 6B). While the protective effects of hucMSC-exo on alleviating weight loss, hematochezia, colon shortening, histopathological injuries, MPO-positive inflammatory cell infiltration and reducing intestinal permeability were all reversed with the application of Wnt-C59 (Figure 6C–I, [Supplementary Figures 6](#) and [7](#)). These indicated that therapeutic effects of hucMSC-exo in experimental colitis depend on the activation of Wnt/ $\beta$ -catenin signaling pathway.

## Repression of Wnt Signaling Pathway Blocked the Effect of hucMSC-Exosomes on Intestinal Stem Cells and Epithelium Regeneration Partially

Wnt signaling pathway activated by hucMSC-exo was inhibited by the application of the Wnt inhibitor Wnt-C59, which was determined by active  $\beta$ -catenin staining as well as the protein expression of WNT2 and  $\beta$ -catenin (Figure 7A and B). Whether the boost effect of hucMSC-exo on ISCs and intestinal epithelium regeneration was blocked by Wnt-C59 accompanied by the reversed therapeutic effect? For further validation, Western blot, IHC and IF staining were performed. Expectedly, the ISCs hallmark protein LGR5 was down-regulated dramatically in DSS+EXO+Wnt-C59 group (Figure 7A). The regeneration ability of intestinal epithelium, as determined by Ki-67 staining and EdU incorporation assay, was inhibited notably by Wnt-C59 (Figure 7C and D, [Supplementary Figure 8A](#) and [B](#)).

## Investigate Potential Specific Components of hucMSC-exo by Public Data Acquisition and Bioinformatics Analysis

To further explore the potential key components of hucMSC-exo, we analyzed and integrated the existing hucMSCs and hucMSC-exo miRNAs expression profile datasets. A specific miRNAs abundance signature was found in hucMSC-exo which was quite different from exosomes derived from any other cells and even hucMSCs (Figure 8A, [Supplementary Table 4](#)). More specifically, the most 2 abundant miRNAs in hucMSCs, *hsa-miR-21-5p* and *hsa-miR-143-3p*, were downregulated in hucMSC-exo, while other miRNAs were upregulated, such as *has-let-7a-5p*, *has-miR-100-5p*, *hsa-let-7f-5p* and so on. That is to say, hucMSC-exo might exert their biological effects by the enrichment or reassembly of specific miRNAs cargos. The most abundant miRNAs overlapped in at least 2 datasets are exhibited in Figure 8B, *hsa-miR-21-5p*, *hsa-let-7a-5p*, *hsa-miR-100-5p* and *hsa-let-7f-5p* were abundant in all three datasets. Functional enrichment analyses of the acquired four miRNAs was further performed based on the target genes predicted by TargetScan, miRDB and TarBase. And a total of 1853 target genes were predicted, among these, 754 target genes for *hsa-miR-21-5p*, 1112 target genes for *hsa-let-7a-5p*, 69 target genes for *hsa-miR-100-5p* and 1066 target genes for *hsa-let-7f-5p* ([Supplementary Table 5](#)). As shown in Figure 8C, these abundant miRNAs involved widely in regeneration or repair related biological processes, such as “apoptotic process”, “positive regulation of cell proliferation”, “cell cycle”, “wound healing” and so on. The possible signaling pathways included Wnt signaling pathway which we had verified above played a pivotal role in mucosal healing triggered by hucMSC-exo (Figure 8D).



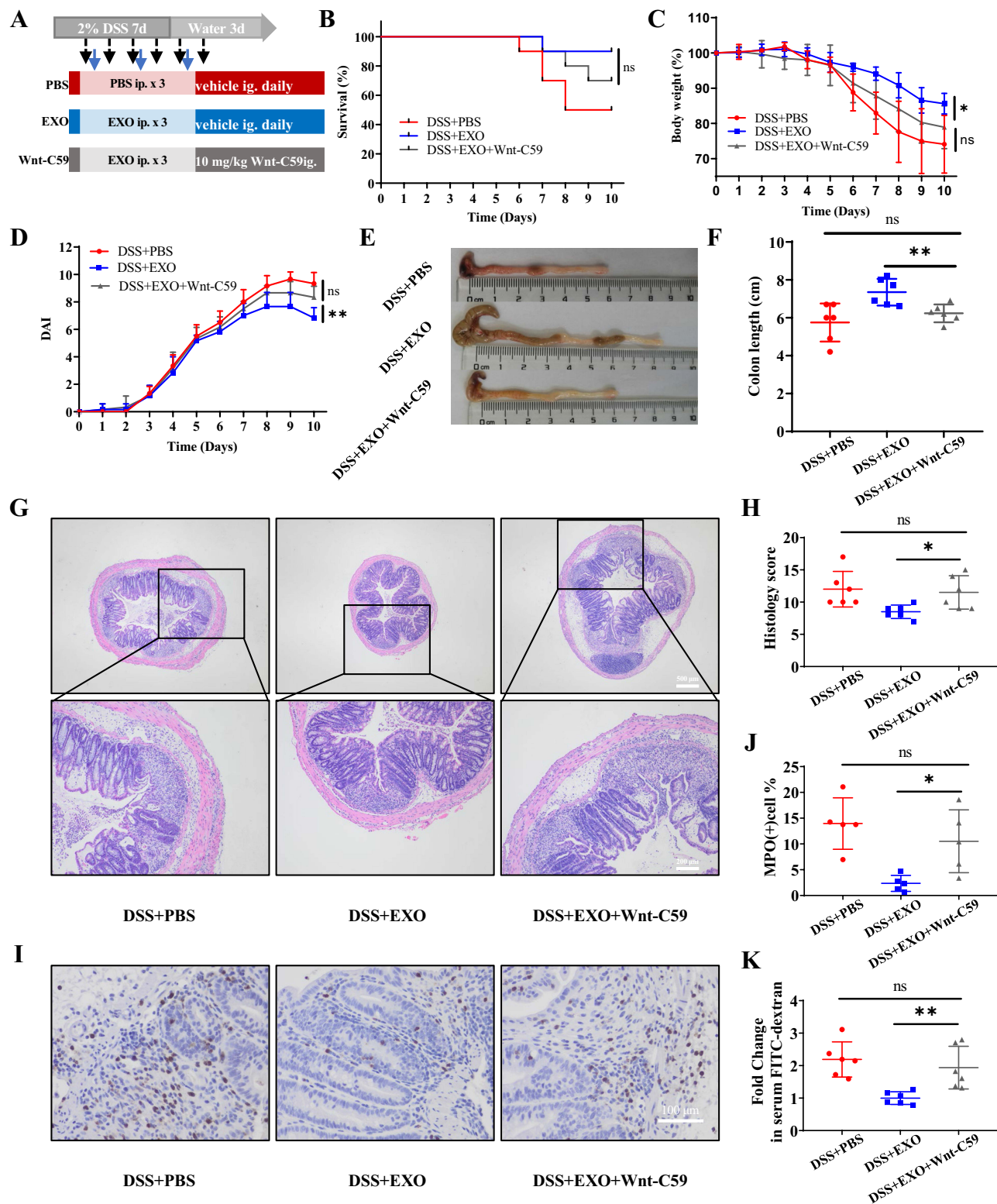


**Figure 6** Wnt-C59 blocked the therapeutic efficacy of hucMSC-exosomes partially. **(A)** Experimental scheme for the pathway inhibited model. **(B–F)** exhibited the survival curves ( $n=10$ ), mice weight, DAI scores, macroscopic images of colonic tissues and colon length of mice in different groups respectively ( $n=6$ ). **(G and H)** H&E staining and corresponding histological scores of mice colon sections ( $n=6$ , scale bar=500  $\mu\text{m}$ , 40 $\times$ ; scale bar=200  $\mu\text{m}$ , 100 $\times$ ). **(I and J)** The neutrophil infiltration in the colon tissues measured by IHC staining of MPO ( $n=5$ , scale bar=100  $\mu\text{m}$ , 400 $\times$ ). **(K)** Fold change in serum FITC-dextran between each group ( $n=6$ ). Data were shown as mean  $\pm$  SD. Mouse survival curves were plotted by the Kaplan–Meier method and analyzed by Log rank test. The Unpaired Student's  $t$ -test was used to compare the variables between two groups.  $P<0.05$  was considered as statistically significant. \* $P<0.05$ , \*\* $P<0.01$  and ns indicates  $P>0.05$ .

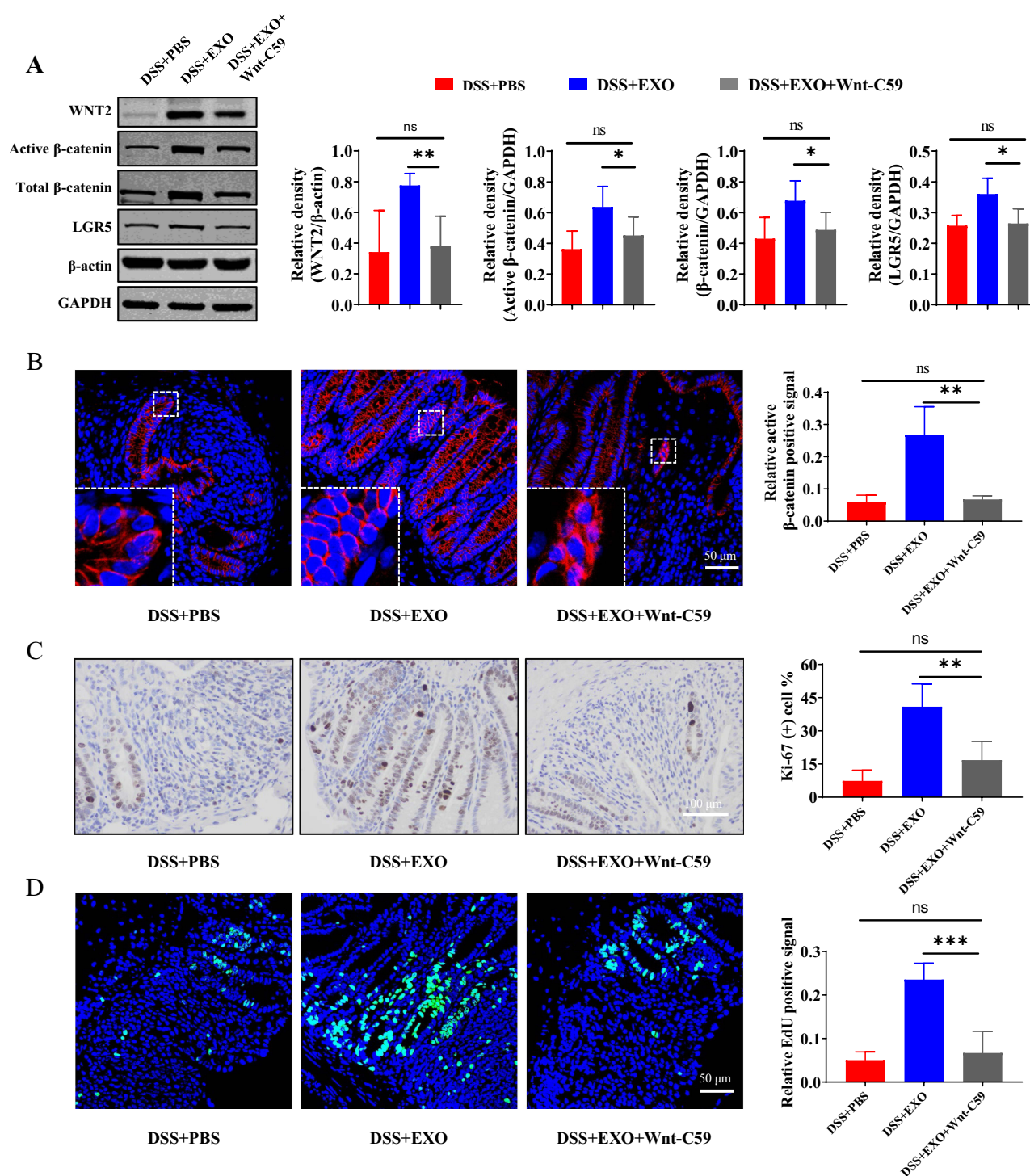


**Figure 7** Wnt-C59 blocked the promoting effects of hucMSC-exosomes on regeneration of ISCs and intestinal epithelium partially. **(A)** Western blot analysis of the protein expression level of WNT2, active  $\beta$ -catenin, total  $\beta$ -catenin and LGR5 in the pathway inhibited model ( $n=5$ , corresponding full-length blots are presented in [Supplementary Figure 4](#)). **(B)** The localization and expression of active  $\beta$ -catenin (red) was analyzed by IF staining of active  $\beta$ -catenin. The purple region produced by the mixture of red and blue (DAPI) was thought to be the place where  $\beta$ -catenin entered the nucleus. The proliferation potential of colon epithelium was measured by IHC staining of Ki-67 (**(C)**  $n=5$ , scale bar=100  $\mu$ m, 400 $\times$ ) and EdU incorporation assay (**(D)**  $n=5$ , scale bar=50  $\mu$ m, 400 $\times$ ). Data were shown as mean  $\pm$  SD. The Mann-Whitney  $U$ -test (non-normal distribution) or Unpaired Student's  $t$ -test (normal distribution) was used to compare the variables between two groups.  $P<0.05$  was considered as statistically significant. \* $P<0.05$ , \*\* $P<0.01$ , \*\*\* $P<0.001$ , ns indicates  $P>0.05$ .



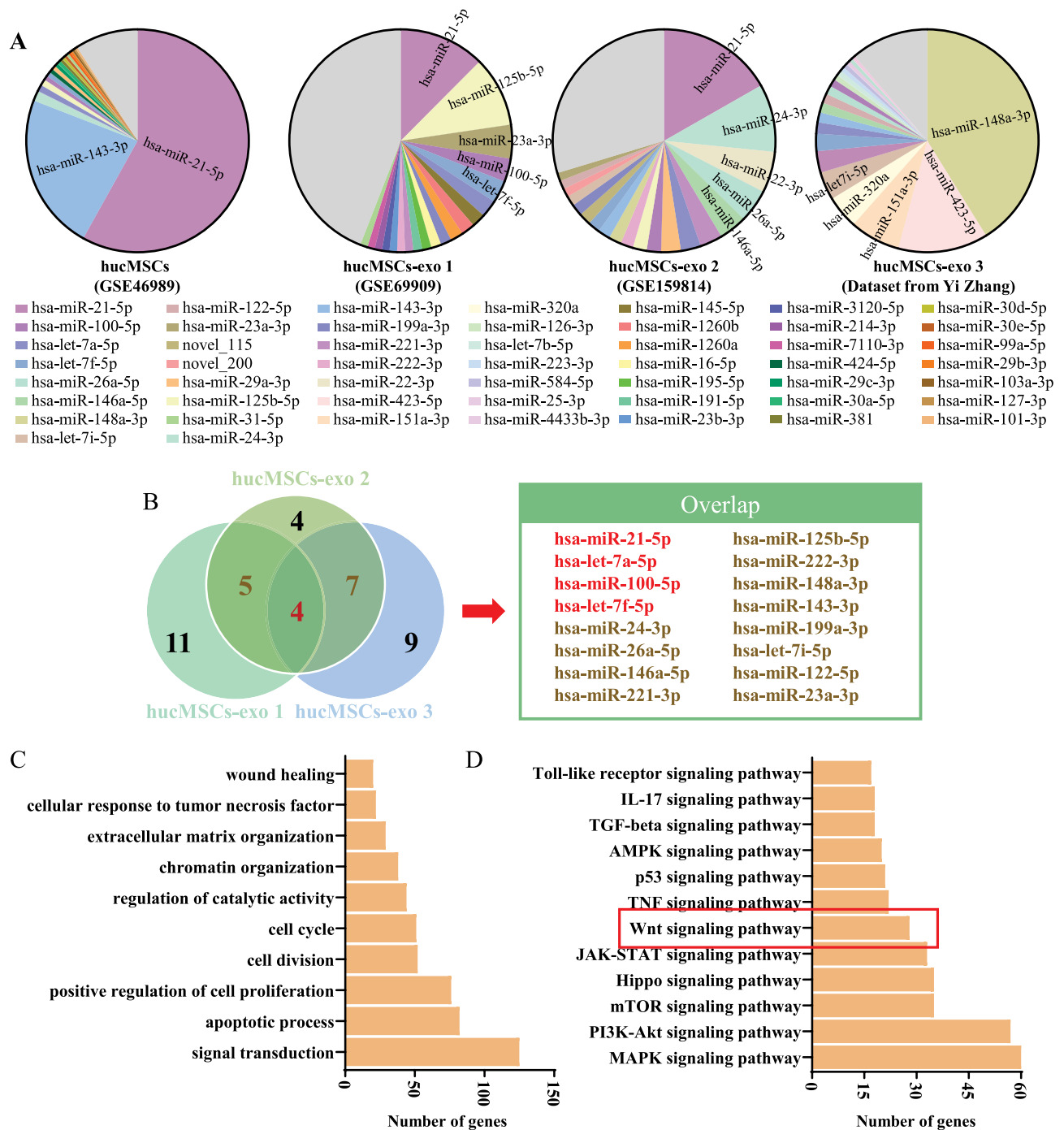


**Figure 8** Identification of hucMSC-exo-specific microRNAs based on public data acquisition and bioinformatic analysis. **(A)** HucMSCs and hucMSC-exo miRNAs abundance analysis using GSE46989, GSE69909 and GSE159814 from the GEO DataSet as well as sequencing data from Yi Zhang. **(B)** Venn diagram for the intersection of the 20 most abundant miRNAs from three different datasets and the overlap miRNAs. **(C)** Gene Ontology analysis of the TargetScan-, miRDB- and TarBase-predicted mRNA targets for the four overlap miRNAs in three datasets. **(D)** KEGG analysis of the predicted mRNA targets.

## Discussion

The inflammatory bowel diseases are chronic idiopathic intestinal disorders with vague etiology at present and gradually increased incidence all over the world.<sup>39</sup> The advent of the precision medicine era for IBD has shifted the therapeutic goal from controlling the disease activity alone to managing other associated problems.<sup>40</sup> Therefore, mucosal healing as a key target for IBD emerged.<sup>3</sup> Encouraging data from ongoing basic studies reveals exosomes-based therapy is a promising therapeutic

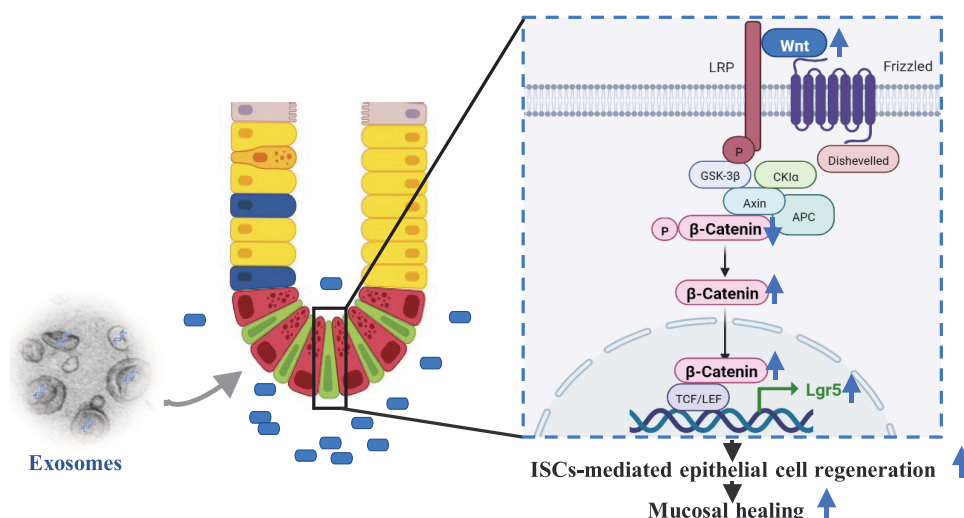


**Figure 9** The schema of hucMSC-exosomes to promote mucosal healing.

approach for IBD, of which exosomes derived from MSCs are an important component.<sup>18,19,41–43</sup> Nevertheless, several issues concerning the mechanisms of action remain unresolved. In this study, DSS- and TNBS-induced colitis model as well as IBD organoid model were constructed to investigate the therapeutic effects of hucMSC-exo on IBD. Here, we found that hucMSC-exo could promote mucosal healing effectively by accelerating the regeneration of Lgr5<sup>+</sup> ISCs and intestinal epithelium after injury. Furthermore, we elucidated the molecular mechanism underlying the efficacy of hucMSC-exo by RNA-sequencing for the first time and corroborated the role of the key signaling pathway rigorously by the inhibition assay. And the potential specific components of hucMSC-exo were identified by public data acquisition and analysis.

Mucosal healing is evolving as a crucial therapeutic goal in IBD; nevertheless, its definition and criteria remain controversial. And several other nomenclatures have to be mentioned, such as histological healing, histological remission and deep remission. Mucosal healing in IBD patients underscores the indispensability of endoscopy beyond all question, depicted as the elimination of mucosal friability, blood, ulcers and erosions in all visualized intestinal segments,<sup>3,40,44</sup> whereas endoscopic remission is not always in line with histologically quiescent diseases.<sup>45</sup> Hence, when defining mucosal healing, the process of histological epithelial healing characterized by the resolution of inflammation, the proliferation and differentiation of epithelium as well as eventual improvement of the mucosal function should be considered, in which neutrophil-free mucosa is undisputed.<sup>40,44</sup> Previous studies have demonstrated that exosomes could be delivered into intestines effectively by intraperitoneal injection and be taken-up by intestinal epithelial cells which provide the basis for the therapeutic effects of exosomes in colitis.<sup>46,47</sup> In this study, hucMSC-exo were subjected to colitis mice intraperitoneally after damage had been induced by DSS or TNBS, which were proved according to the increased DAI scores and the characteristics of colitis model,<sup>48</sup> to estimate the therapeutic effects. And we found that hucMSC-exo could endow colitis mice decreased inflammatory cell infiltration, reduced destruction of crypt and improved epithelial integrity, which were similar to previous studies.<sup>18,28,49</sup> Not only that, our previous research demonstrated its protective effects on intestinal barrier function in detail.<sup>19</sup> These findings indicated that hucMSC-exo could promote mucosal healing effectively.

The intact barrier function of gut epithelium is the structural basis of mucosal healing.<sup>8</sup> And the maintenance of the integrity of epithelial barrier is highly dependent on a robust engine for intestinal turnover, in which Lgr5<sup>+</sup> crypt base columnar cells as typical ISCs drive the immense continuous replenishment of new epithelium.<sup>38,50,51</sup> Consequently, the regeneration capability of ISCs is essential for mucosal healing in IBD. Substantial evidences have revealed that MSCs could accelerate the regeneration of ISCs in experimental colitis mice.<sup>27,52</sup> Yu et al indicated that exosomes isolated from human adipose derived MSCs increased the mean fluorescence intensity of the specific ISCs marker Lgr5.<sup>42</sup> Although there was a dearth of formal proof providing by Lgr5-EGFP-IRES-CreERT2 mice, further credence was lent to the role of hucMSC-exo in the regeneration of ISCs to some extent by detecting the mRNA and protein expression of Lgr5

quantitatively in our study. We also found that hucMSC-exo could endow epithelium with greater proliferation potential, featured with an impressive increase in Ki-67 positive cells and EdU incorporation.

In recent years, the groundbreaking organoid technology has opened new horizons in studying the biology of human tissues *ex vivo*. Colonic and intestinal organoids self-assembled from Lgr5<sup>+</sup> ISC or pluripotent stem cells provide a fascinating opportunity to mimic IBD.<sup>53</sup> Insulin-like growth factor-1, a well-known agonist for damage repair and tissue regeneration, was proved to be beneficial for the growth and budding of colonic organoids in a dose-dependent manner.<sup>27</sup> Substantial traditional Chinese medicine and other bioactive substances were also verified to be efficacious for intestinal organoids to resist injury induced by pro-inflammatory cytokines TNF- $\alpha$  or INF- $\gamma$ .<sup>25,54–56</sup> In our present study, great effort was devoted to showcase the enormous potential role of hucMSC-exo in ISCs regeneration vividly, characterized by the increased growth rate, budding rate and average buddings number.

The fate of ISCs is governed by a sophisticated signaling network encompassing Wnt, Notch, Hippo, EGF, as well as BMP signaling to safeguard tissue integrity and orchestrate homeostasis after injury, and the canonical Wnt signaling pathway seems to be the workhorse among all of them.<sup>37,57</sup> Christine Harnack et al demonstrated that R-spondin 3, a powerful agonist for Wnt signaling pathway, promoted stem cell recovery and epithelial regeneration in the colon,<sup>58</sup> which is always supplemented to the cocktail of growth factor as an essential component for the organoid culture system. Plant extract glucomannan was turned out to be a potential fuel to promote ISCs mediated epithelial regeneration via the Wnt/ $\beta$ -catenin pathway.<sup>30</sup> Whether the Wnt/ $\beta$ -Catenin pathway was implicated in the ISCs regeneration triggered by hucMSC-exo? In our study, RNA-seq analysis verified this hypothesis, which was consistent with the test results of Wnt ligand and  $\beta$ -catenin *in vivo*. Not only that, the Wnt antagonist Wnt-C59 confirmed the dominating role of Wnt signaling pathway in mucosal healing expedited by hucMSC-exo.

Emerging studies have demonstrated that exosomes exert biological effects mainly through the delivery of their specific payloads, such as proteins and miRNAs, especially miRNAs. Many different miRNAs have been demonstrated as the key component of exosomes which could play critical roles in IBD by regulating diverse biological processes, such as *miR-216a-5p* for macrophage polarization,<sup>59</sup> *miR-378a-5p* for macrophage pyroptosis,<sup>17</sup> *miR-302d-3p* for lymphangiogenesis,<sup>60</sup> and so on. These also tell us that the functional component of exosomes is not restricted to one certain miRNAs. Furthermore, miRNA abundance signature and bioinformatics analysis revealed that *hsa-miR-21-5p*, the most abundant miRNA in hucMSCs, which is highly expressed in IBD and has an essential promoting effect on the initiation and progression of IBD,<sup>61</sup> was downregulated in hucMSC-exo significantly, while *has-let-7a-5p*, *has-miR-100-5p* and *hsa-let-7f-5p* were upregulated and expressed stably in hucMSC-exo. Interestingly, many researches have demonstrated that *let-7* miRNAs are critical for ameliorating intestinal inflammation, promoting Paneth cell differentiation and maintaining intestinal epithelial homeostasis.<sup>62–64</sup> As for *miR-100*,<sup>65</sup> Lu et al have verified that it could repress Wnt/ $\beta$ -catenin negative regulators, DKK1 and zinc and ring finger 3 (ZNRF3), resulting in increased Wnt signaling; Cao et al found *miR-100* derived from ReN cells exosome-mimetic nanovesicle could promote dermal papilla cell proliferation by Wnt signaling pathway, indicating that *miR-100* might also be one positive regulator of intestinal epithelium proliferation.<sup>66</sup> In summary, hucMSC-exo might reassemble the potential salutary and noxious miRNAs cargos, resulting in the activated Wnt signaling pathway, to promote mucosal healing in IBD.

In this study, we focused on the role of hucMSC-exo in Lgr5<sup>+</sup> ISCs regeneration and investigate the underlying mechanism based on transcriptome sequencing and pathway inhibition experiment. Subsequently, we tried to profile the whole miRNA landscape by analyzing and integrating the existing miRNA expression profile datasets and identified several miRNAs abundant in all three datasets. Excitingly, these abundant miRNAs involved widely in regeneration or repair related biological processes and Wnt signaling pathway may participate in the above processes, which were consistent with the role and mechanism of hucMSC-exo in mucosal healing in IBD that we elucidated above. These suggested that the reassembly of specific exosomes miRNAs cargos targeting on Wnt signaling pathway might be a promising research direction in IBD.

Nonetheless, it should also be acknowledged that there may be some potential limitations in this study. The effect of hucMSC-exo on ISCs regeneration was explored only at Lgr5 mRNA and protein expression level, it is lack of other evidence for ISCs regeneration. In addition, in-depth mechanism still needs to be investigated, such as which kind of intestinal Wnt-secreting cells and specific Wnt pathway components were modulated by hucMSC-exo, how do they regulate? This will be one of the research emphases in our further study.

## Conclusion

In conclusion, our study demonstrated that hucMSC-exo could expedite the regeneration of ISCs and intestinal epithelium, then promote mucosal healing after injury via transferring key miRNAs. And that facilitation was dependent on the activation of Wnt/ $\beta$ -catenin pathway partially (Figure 9). This may allow novel insights into regenerative medicine applications for IBD.

## Abbreviations

BMP, bone morphogenetic protein; DAI, disease activity index; DEGs, differentially expressed genes; DPBS, Dulbecco's phosphate-buffered saline; DSS, Dextran sulfate sodium; EGF, epidermal growth factor; Exo, Exosomes; GCDR, Gentle Cell Dissociation Reagent; GSEA, Gene set enrichment analysis; H&E, hematoxylin and eosin; hucMSCs, human umbilical cord mesenchymal stem cells; IBD, inflammatory bowel diseases; IF, immunofluorescence; IHC, immunohistochemical; IL, interleukin; INF, interferon; ISCs, intestinal stem cells; Lgr5, leucine-rich repeat-containing G-protein coupled receptor 5; MPO, myeloperoxidase; SPF, specific-pathogen-free; TEM, transmission electron microscopy; TNBS, 2,4,6-trinitrobenzenesulfonic acid; TNF, tumor necrosis factor; ZNRF3, zinc and ring finger 3.

## Data Sharing Statement

The data that support the findings of this study are available from the corresponding author upon reasonable request.

## Ethics Approval and Informed Consent

This study was approved by the Research and Ethical Committee of the Second Hospital of Hebei Medical University (No.2022-AE249). All procedures followed the relevant provisions of China's Guidelines for the Ethical Review of Laboratory Animal Welfare.

## Acknowledgments

The authors acknowledge the support of Dr. Jun Yu (The Chinese University of Hong Kong) for supervising this study.

## Funding

This work was supported by grants from Hebei provincial Excellent Medical Talents Project funded by government (2021), the National Natural Science Foundation of China (No. 82070563) and the Natural Science Foundation of Hebei Province (No. H2020206497).

## Disclosure

The authors declare no potential conflicts of interest in this work.

## References

1. Chang JT. Pathophysiology of inflammatory bowel diseases. *N Engl J Med*. 2020;383(27):2652–2664. doi:10.1056/NEJMra2002697
2. Shouval DS, Rufo PA. The role of environmental factors in the pathogenesis of inflammatory bowel diseases, A review. *JAMA Pediatr*. 2017;171(10):999–1005. doi:10.1001/jamapediatrics.2017.2571
3. Pineton de Chambrun G, Peyrin-Biroulet L, Lemann M, Colombel JF. Clinical implications of mucosal healing for the management of IBD. *Nat Rev Gastroenterol Hepatol*. 2010;7(1):15–29. doi:10.1038/nrgastro.2009.203
4. Panaccione R, Ghosh S, Middleton S, et al. Combination therapy with infliximab and azathioprine is superior to monotherapy with either agent in ulcerative colitis. *Gastroenterology*. 2014;146(2):392–400 e393. doi:10.1053/j.gastro.2013.10.052
5. Sandborn WJ, Su C, Sands BE, et al. Tofacitinib as induction and maintenance therapy for ulcerative colitis. *N Engl J Med*. 2017;376(18):1723–1736. doi:10.1056/NEJMoa1606910
6. Sands BE, Peyrin-Biroulet L, Loftus EV Jr, et al. Vedolizumab versus adalimumab for moderate-to-severe ulcerative colitis. *N Engl J Med*. 2019;381(13):1215–1226. doi:10.1056/NEJMoa1905725
7. Sands BE, Sandborn WJ, Panaccione R, et al. Ustekinumab as induction and maintenance therapy for ulcerative colitis. *N Engl J Med*. 2019;381(13):1201–1214. doi:10.1056/NEJMoa1900750
8. Neurath MF, Travis SP. Mucosal healing in inflammatory bowel diseases, a systematic review. *Gut*. 2012;61(11):1619–1635. doi:10.1136/gutjnl-2012-302830

9. Satija NK, Singh VK, Verma YK, et al. Mesenchymal stem cell-based therapy, a new paradigm in regenerative medicine. *J Cell Mol Med*. 2009;13(11–12):4385–4402. doi:10.1111/j.1582-4934.2009.00857.x
10. Song N, Scholtemeijer M, Shah K. Mesenchymal stem cell immunomodulation, mechanisms and therapeutic potential. *Trends Pharmacol Sci*. 2020;41(9):653–664. doi:10.1016/j.tips.2020.06.009
11. Jasim SA, Yumashev AV, Abdelbasset WK, et al. Shining the light on clinical application of mesenchymal stem cell therapy in autoimmune diseases. *Stem Cell Res Ther*. 2022;13(1):101. doi:10.1186/s13287-022-02782-7
12. Panes J, Garcia-Olmo D, Van Assche G, et al. Expanded allogeneic adipose-derived mesenchymal stem cells (Cx601) for complex perianal fistulas in Crohn's disease, a Phase 3 randomised, double-blind controlled trial. *Lancet*. 2016;388(10051):1281–1290. doi:10.1016/S0140-6736(16)31203-X
13. Lötvall J, Hill AF, Hochberg F, et al. Minimal experimental requirements for definition of extracellular vesicles and their functions, a position statement from the international society for extracellular vesicles. *J Extracell Vesicles*. 2014;3:26913. doi:10.3402/jev.v3.26913
14. Kalluri R, LeBleu VS. The biology, function, and biomedical applications of exosomes. *Science*. 2020;367(6478). doi:10.1126/science.aau6977
15. Ma ZJ, Wang YH, Li ZG, et al. Immunosuppressive effect of exosomes from mesenchymal stromal cells in defined medium on experimental colitis. *Int J Stem Cells*. 2019;12(3):440–448. doi:10.15283/ijsc.18139
16. Mao F, Wu Y, Tang X, et al. Exosomes derived from human umbilical cord mesenchymal stem cells relieve inflammatory bowel disease in mice. *Biomed Res Int*. 2017;2017:5356760. doi:10.1155/2017/5356760
17. Cai X, Zhang ZY, Yuan JT, et al. hucMSC-derived exosomes attenuate colitis by regulating macrophage pyroptosis via the miR-378a-5p/NLRP3 axis. *Stem Cell Res Ther*. 2021;12(1):416. doi:10.1186/s13287-021-02492-6
18. Joo H, Oh MK, Kang JY, et al. Extracellular vesicles from thapsigargin-treated mesenchymal stem cells ameliorated experimental colitis via enhanced immunomodulatory properties. *Biomedicines*. 2021;9(2):209. doi:10.3390/biomedicines9020209
19. Yang S, Liang X, Song J, et al. A novel therapeutic approach for inflammatory bowel disease by exosomes derived from human umbilical cord mesenchymal stem cells to repair intestinal barrier via TSG-6. *Stem Cell Res Ther*. 2021;12(1):315. doi:10.1186/s13287-021-02404-8
20. Wu H, Xie S, Miao J, et al. Lactobacillus reuteri maintains intestinal epithelial regeneration and repairs damaged intestinal mucosa. *Gut Microbes*. 2020;11(4):997–1014. doi:10.1080/19490976.2020.1734423
21. Wang L, Xie H, Liao Q, et al. rsJ16 Protects against DSS-Induced Colitis by Inhibiting the PPAR- $\alpha$  Signaling Pathway. *Theranostics*. 2017; 7(14):3446–3460. doi:10.7150/thno.20359
22. Sato T, Vries RG, Snippert HJ, et al. Single Lgr5 stem cells build crypt-villus structures in vitro without a mesenchymal niche. *Nature*. 2009;459(7244):262–265. doi:10.1038/nature07935
23. Gaowa A, Park EJ, Kawamoto E, Qin Y, Shimaoka M. Recombinant soluble thrombomodulin accelerates epithelial stem cell proliferation in mouse intestinal organoids and promotes the mucosal healing in colitis. *J Gastroenterol Hepatol*. 2021;36(11):3149–3157. doi:10.1111/jgh.15656
24. Goodman WA, Basavarajappa SC, Liu AR, Rodriguez FDS, Mathes T, Ramakrishnan P. Sam68 contributes to intestinal inflammation in experimental and human colitis. *Cell Mol Life Sci*. 2021;78(23):7635–7648. doi:10.1007/s00018-021-03976-7
25. Yu W, Wang G, Lu C, et al. Pharmacological mechanism of Shenlingbaizhu formula against experimental colitis. *Phytomedicine*. 2022;98:153961. doi:10.1016/j.phymed.2022.153961
26. Dieleman LA, Palmen MJ, Akol H, et al. Chronic experimental colitis induced by dextran sulphate sodium (DSS) is characterized by Th1 and Th2 cytokines. *Clin Exp Immunol*. 1998;114(3):385–391. doi:10.1046/j.1365-2249.1998.00728.x
27. Xu J, Wang X, Chen J, et al. Embryonic stem cell-derived mesenchymal stem cells promote colon epithelial integrity and regeneration by elevating circulating IGF-1 in colitis mice. *Theranostics*. 2020;10(26):12204–12222. doi:10.7150/thno.47683
28. Duan L, Huang H, Zhao X, et al. Extracellular vesicles derived from human placental mesenchymal stem cells alleviate experimental colitis in mice by inhibiting inflammation and oxidative stress. *Int J Mol Med*. 2020;46(4):1551–1561. doi:10.3892/ijmm.2020.4679
29. Lee YS, Kim TY, Kim Y, et al. Microbiota-derived lactate accelerates intestinal stem-cell-mediated epithelial development. *Cell Host Microbe*. 2018;24(6):833–846 e836. doi:10.1016/j.chom.2018.11.002
30. Zhang D, Zhou X, Liu L, et al. Glucomannan from aloe vera gel promotes intestinal stem cell-mediated epithelial regeneration via the Wnt/ $\beta$ -catenin pathway. *J Agric Food Chem*. 2021;69(36):10581–10591. doi:10.1021/acs.jafc.1c03814
31. Liu W, Zhou N, Liu Y, et al. Mesenchymal stem cell exosome-derived miR-223 alleviates acute graft-versus-host disease via reducing the migration of donor T cells. *Stem Cell Res Ther*. 2021;12(1):153. doi:10.1186/s13287-021-02159-2
32. Agarwal V, Bell GW, Nam JW, Bartel DP. Predicting effective microRNA target sites in mammalian mRNAs. *Elife*. 2015;2015:4.
33. Chen Y, Wang X. miRDB, an online database for prediction of functional microRNA targets. *Nucleic Acids Res*. 2020;48(D1):D127–D131. doi:10.1093/nar/gkz757
34. Karagkouni D, Paraskevopoulou MD, Chatzopoulos S, et al. DIANA-TarBase v8, a decade-long collection of experimentally supported miRNA-gene interactions. *Nucleic Acids Res*. 2018;46(D1):D239–D245. doi:10.1093/nar/gkx1141
35. Sherman BT, Hao M, Qiu J, et al. DAVID, a web server for functional enrichment analysis and functional annotation of gene lists (2021 update). *Nucleic Acids Res*. 2022;50(W1):W216–221. doi:10.1093/nar/gkac194
36. Huang da W, Sherman BT, Lempicki RA. Systematic and integrative analysis of large gene lists using DAVID bioinformatics resources. *Nat Protoc*. 2009;4(1):44–57. doi:10.1038/nprot.2008.211
37. Clevers H, Loh KM, Nusse R. Stem cell signaling. An integral program for tissue renewal and regeneration, Wnt signaling and stem cell control. *Science*. 2014;346(6205):1248012. doi:10.1126/science.1248012
38. Beumer J, Clevers H. Cell fate specification and differentiation in the adult mammalian intestine. *Nat Rev Mol Cell Biol*. 2021;22(1):39–53. doi:10.1038/s41580-020-0278-0
39. Ng SC, Shi HY, Hamidi N, et al. Worldwide incidence and prevalence of inflammatory bowel disease in the 21st century, a systematic review of population-based studies. *Lancet*. 2017;390(10114):2769–2778. doi:10.1016/S0140-6736(17)32448-0
40. Moriichi K, Fujiya M, Okumura T. The endoscopic diagnosis of mucosal healing and deep remission in inflammatory bowel disease. *Dig Endosc*. 2021;33(7):1008–1023. doi:10.1111/den.13863
41. Gu L, Ren F, Fang X, Yuan L, Liu G, Wang S. Exosomal MicroRNA-181a derived from mesenchymal stem cells improves gut microbiota composition, barrier function, and inflammatory status in an experimental colitis model. *Front Med*. 2021;8:660614. doi:10.3389/fmed.2021.660614
42. Yu H, Yang X, Xiao X, et al. Human adipose mesenchymal stem cell-derived exosomes protect mice from DSS-induced inflammatory bowel disease by promoting intestinal-stem-cell and epithelial regeneration. *Aging Dis*. 2021;12(6):1423–1437. doi:10.14336/AD.2021.0601



43. Yu T, Chu S, Liu X, et al. Extracellular vesicles derived from EphB2-overexpressing bone marrow mesenchymal stem cells ameliorate DSS-induced colitis by modulating immune balance. *Stem Cell Res Ther.* 2021;12(1):181. doi:10.1186/s13287-021-02232-w
44. Gui X, Bazarova A, Del Amor R, et al. PICaSSO Histologic Remission Index (PHRI) in ulcerative colitis, development of a novel simplified histological score for monitoring mucosal healing and predicting clinical outcomes and its applicability in an artificial intelligence system. *Gut.* 2022;71(5):889–898. doi:10.1136/gutjnl-2021-326376
45. Bryant RV, Burger DC, Delo J, et al. Beyond endoscopic mucosal healing in UC, histological remission better predicts corticosteroid use and hospitalisation over 6 years of follow-up. *Gut.* 2016;65(3):408–414. doi:10.1136/gutjnl-2015-309598
46. Barnhoorn MC, Plug L, Jonge E, et al. Mesenchymal stromal cell-derived exosomes contribute to epithelial regeneration in experimental inflammatory bowel disease. *Cell Mol Gastroenterol Hepatol.* 2020;9(4):715–717.e718. doi:10.1016/j.jcmgh.2020.01.007
47. Zhou X, Li Z, Sun W, Yang G, Xing C, Yuan L. Delivery efficacy differences of intravenous and intraperitoneal injection of exosomes, perspectives from tracking dye labeled and MiRNA encapsulated exosomes. *Curr Drug Deliv.* 2020;17(3):186–194. doi:10.2174/1567201817666200122163251
48. Cooper HS, Murthy SN, Shah RS, Sedergran DJ. Clinicopathologic study of dextran sulfate sodium experimental murine colitis. *Lab Invest.* 1993;69(2):238–249.
49. Heidari N, Abbasi-Kenarsari H, Namaki S, et al. Adipose-derived mesenchymal stem cell-secreted exosome alleviates dextran sulfate sodium-induced acute colitis by Treg cell induction and inflammatory cytokine reduction. *J Cell Physiol.* 2021;236(8):5906–5920. doi:10.1002/jcp.30275
50. Andersson-Rolf A, Zilbauer M, Koo BK, Clevers H. Stem cells in repair of gastrointestinal Epithelia. *Physiology.* 2017;32(4):278–289. doi:10.1152/physiol.00005.2017
51. Gehart H, Clevers H. Tales from the crypt, new insights into intestinal stem cells. *Nat Rev Gastroenterol Hepatol.* 2019;16(1):19–34. doi:10.1038/s41575-018-0081-y
52. Lim JY, Kim BS, Ryu DB, Kim TW, Park G, Min CK. The therapeutic efficacy of mesenchymal stromal cells on experimental colitis was improved by the IFN-gamma and poly(I:C) priming through promoting the expression of indoleamine 2,3-dioxygenase. *Stem Cell Res Ther.* 2021;12(1):37. doi:10.1186/s13287-020-02087-7
53. Fujii M, Sato T. Somatic cell-derived organoids as prototypes of human epithelial tissues and diseases. *Nat Mater.* 2021;20(2):156–169. doi:10.1038/s41563-020-0754-0
54. Yan J, Yu W, Lu C, et al. The pharmacological mechanism of guchangzhixie capsule against experimental colitis. *Front Pharmacol.* 2021;12:762603. doi:10.3389/fphar.2021.762603
55. Yu W, Cheng H, Zhu B, Yan J. Network pharmacology-based validation of the efficacy of huiyangjiuji decoction in the treatment of experimental colitis. *Front Pharmacol.* 2021;12:666432. doi:10.3389/fphar.2021.666432
56. Tak LJ, Kim HY, Ham WK, et al. Superoxide dismutase 3-transduced mesenchymal stem cells preserve epithelial tight junction barrier in murine colitis and attenuate inflammatory damage in epithelial organoids. *Int J Mol Sci.* 2021;22(12). doi:10.3390/ijms22126431
57. Hageman JH, Heinz MC, Kretschmar K, van der Vaart J, Clevers H, Snippert HJG. Intestinal regeneration, regulation by the microenvironment. *Dev Cell.* 2020;54(4):435–446. doi:10.1016/j.devcel.2020.07.009
58. Harnack C, Berger H, Antanaviciute A, et al. R-spondin 3 promotes stem cell recovery and epithelial regeneration in the colon. *Nat Commun.* 2019;10(1):4368. doi:10.1038/s41467-019-12349-5
59. Qian W, Huang L, Xu Y, et al. Hypoxic ASCs-derived exosomes attenuate colitis by regulating macrophage polarization via miR-216a-5p/HMGB1 axis. *Inflamm Bowel Dis.* 2023;29(4):602–619. doi:10.1093/ibd/izac225
60. Zhang L, Yuan J, Kofi Wiredu Ocansey D, et al. Exosomes derived from human umbilical cord mesenchymal stem cells regulate lymphangiogenesis via the miR-302d-3p/VEGFR3/AKT axis to ameliorate inflammatory bowel disease. *Int Immunopharmacol.* 2022;110:109066. doi:10.1016/j.intimp.2022.109066
61. Johnston DGW, Williams MA, Thaiss CA, et al. Loss of MicroRNA-21 influences the gut microbiota, causing reduced susceptibility in a murine model of colitis. *J Crohns Colitis.* 2018;12(7):835–848. doi:10.1093/ecco-jcc/jjy038
62. Guo Z, Cai X, Guo X, et al. Let-7b ameliorates Crohn's disease-associated adherent-invasive E coli induced intestinal inflammation via modulating Toll-Like Receptor 4 expression in intestinal epithelial cells. *Biochem Pharmacol.* 2018;156:196–203. doi:10.1016/j.bcp.2018.08.029
63. Reif S, Elbaum-Shiff Y, Koroukhov N, Shilo I, Musseri M, Golan-Gerstl R. Cow and human milk-derived exosomes ameliorate colitis in DSS murine model. *Nutrients.* 2020;12(9):2589. doi:10.3390/nu12092589
64. Madison BB, Liu Q, Zhong X, et al. LIN28B promotes growth and tumorigenesis of the intestinal epithelium via Let-7. *Genes Dev.* 2013;27(20):2233–2245. doi:10.1101/gad.224659.113
65. Lu Y, Zhao X, Liu Q, et al. lncRNA MIR100HG-derived miR-100 and miR-125b mediate cetuximab resistance via Wnt/ $\beta$ -catenin signaling. *Nat Med.* 2017;23(11):1331–1341. doi:10.1038/nm.4424
66. Cao L, Tian T, Huang Y, et al. Neural progenitor cell-derived nanovesicles promote hair follicle growth via miR-100. *J Nanobiotechnology.* 2021;19(1):20. doi:10.1186/s12951-020-00757-5